MicroRNA-21 targets the vitamin D-dependent antimicrobial pathway in leprosy

Philip T. Liu, Matthew Wheelwright, Rosane Teles, Evangelia Komisopoulou, Kristina Edfeldt, Benjamin Ferguson, Manali D. Mehta, Aria Vazirnia, Thomas H. Rea, Euzenir N. Sarno, Thomas G. Graeber, and Robert L. Modlin

Supplemental Figures

Supplemental Text

Supplemental Methods

Supplemental References

Supplemental Figure 1

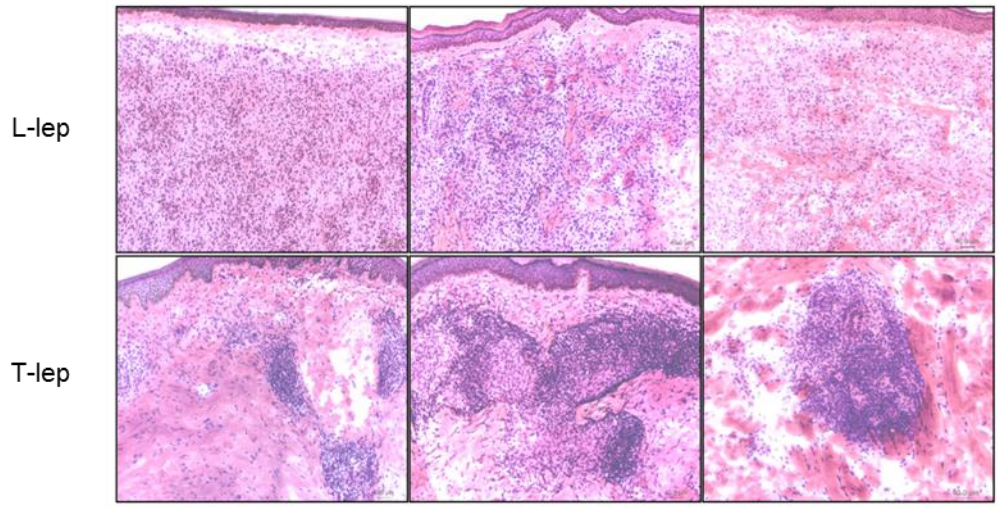

Supplemental Figure 1. Histology of leprosy skin biopsy specimens. Representative hematoxylin and eosin (H&E) stain for L-lep and T-lep skin biopsy specimens used for microarray and qPCR analysis.

Supplemental Figure 2

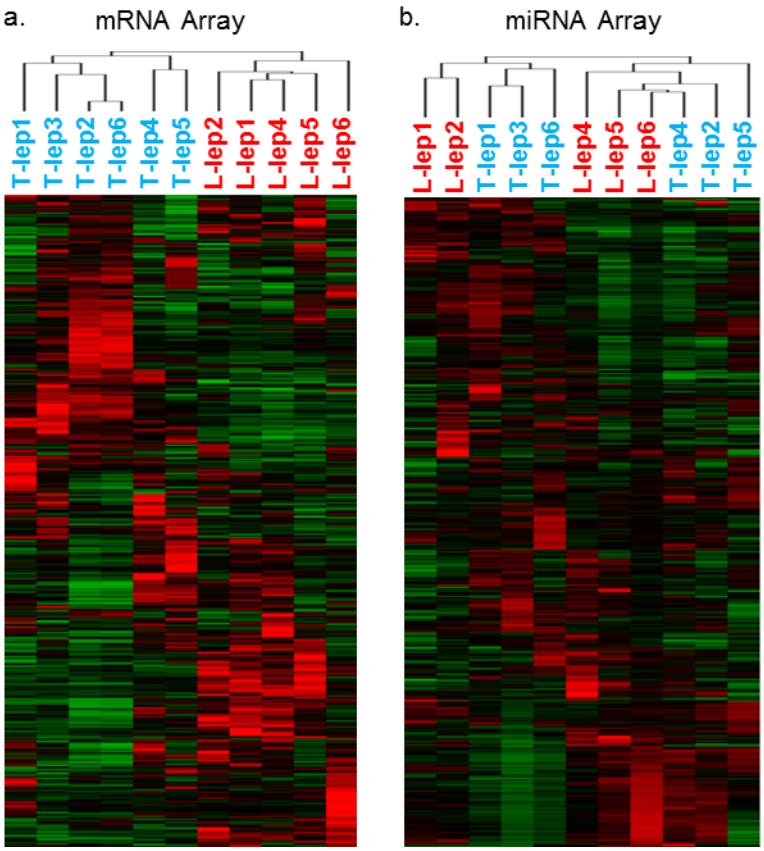

Supplemental Figure 2. mRNA and miRNA expression profile in leprosy skin biopsy specimens. Hierarchical clustering analysis of (**a**) mRNA and (**b**) miRNA microarrays performed on total RNA extracted from six T-lep and five L-lep skin biopsy specimens.

Supplemental Figure 3

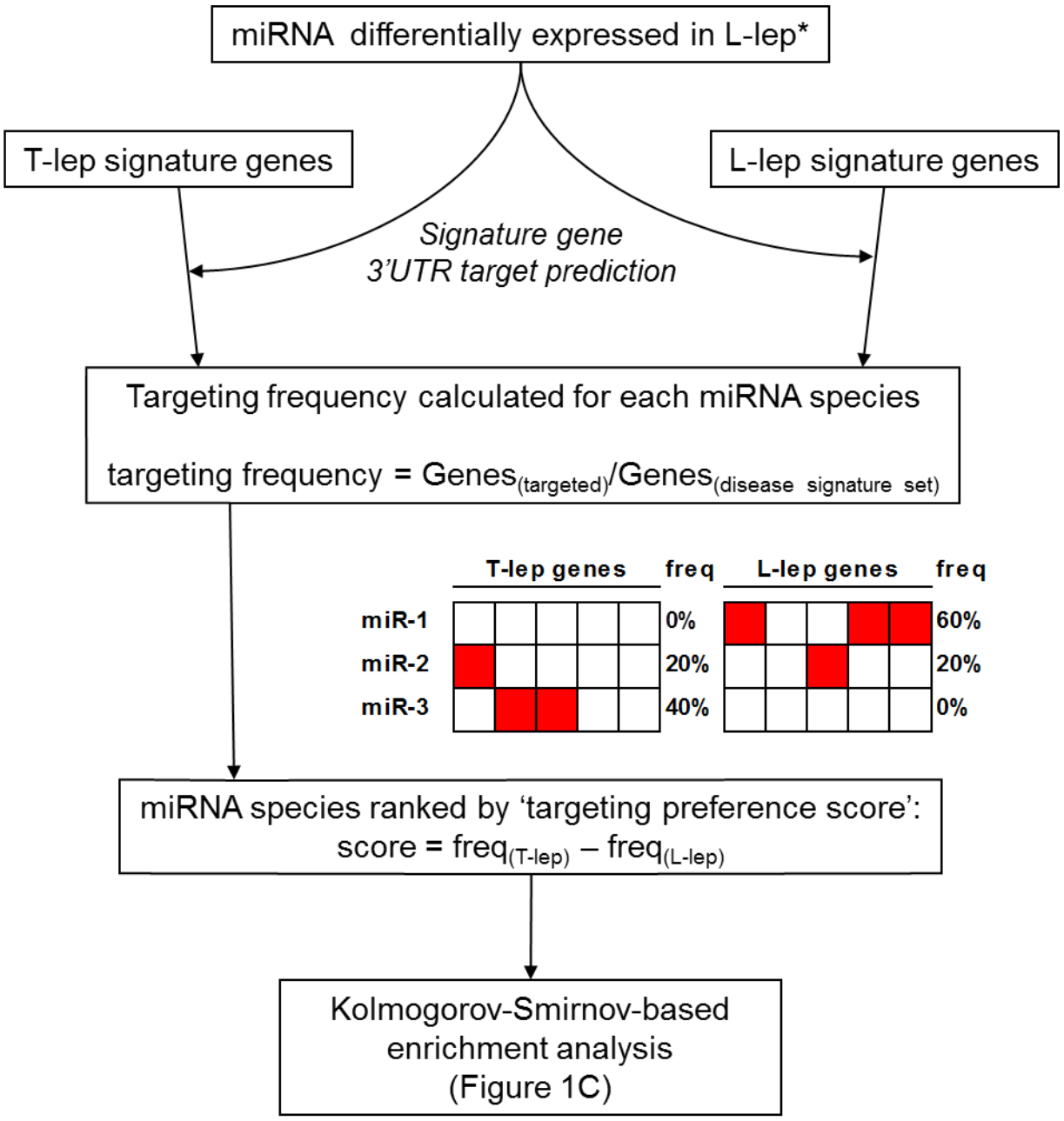

*T-lep specific miRNA were not included in analysis due to lack of statistical power from only two probes.

Supplemental Figure 3. Schematic of targeting enrichment analysis.

Supplemental Figure 4

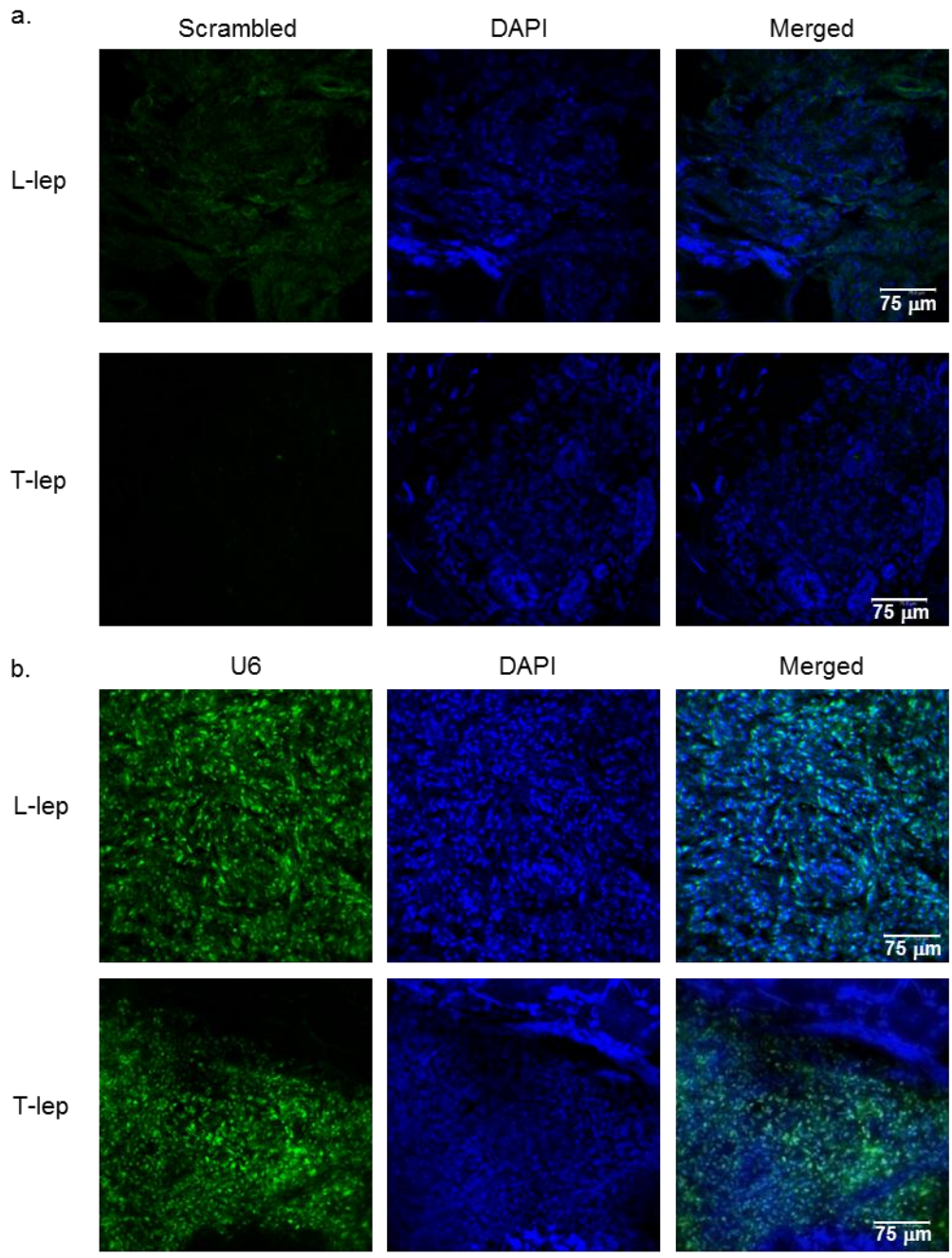

Supplemental Figure 4. *In situ* hybridization for detection of miRNA in leprosy skin biopsy specimens. Representative experiments of L-lep and T-lep skin biopsy specimens labeled with either the (**a**) scrambled negative control or (**b**) positive control oligo for the U6 non-coding small nuclear RNA (U6) using fluorescent *in situ* hybridization detected by confocal microscopy. Data is representative of three individual donors.

Supplemental Figure 5

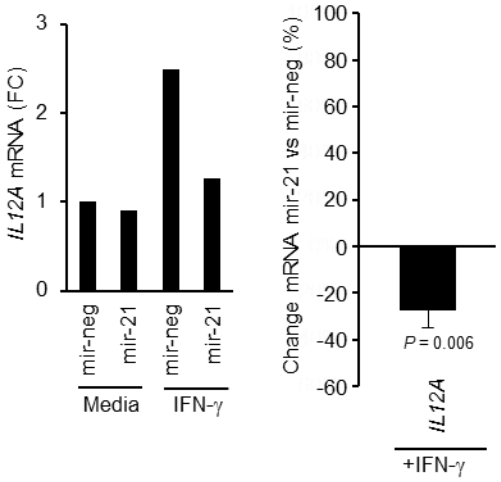

Supplemental Figure 5. Effects of hsa-mir-21 overexpression on the innate immune response. *IL12A* mRNA induction by IFN-γ following transfection of a non-targeting control oligo (mir-neg) or hsa-mir-21 mature oligo (mir-21) into primary human monocytes detected by qPCR. Data shown is representative experiment (left panel) and a summary of all experiments, shown as mean percent change (right panel) ± SEM, $n = 5$.

Supplemental Figure 6

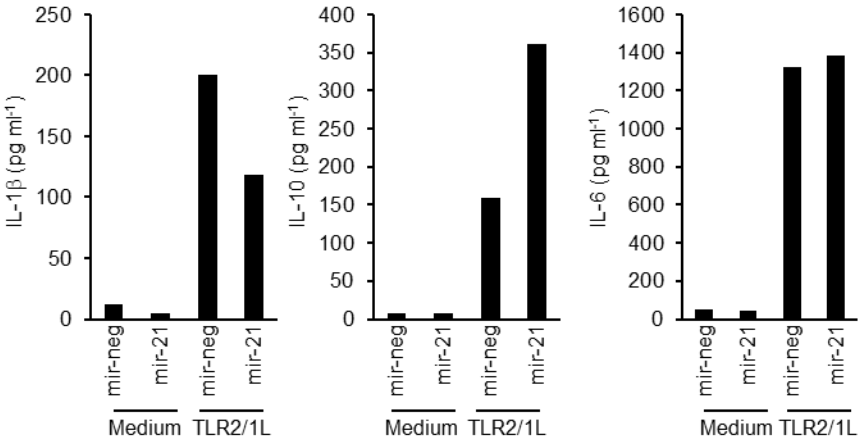

Supplemental Figure 6. Effects of hsa-mir-21 overexpression on the innate immune triggered cytokine response. IL-1β, IL-10 and IL-6 levels in the culture supernatants of mir-neg or mir-21 transfected cells followed by TLR2/1L stimulation as detected by CBA. Data shown is representative experiment of four to five independent donors.

Supplemental Figure 7

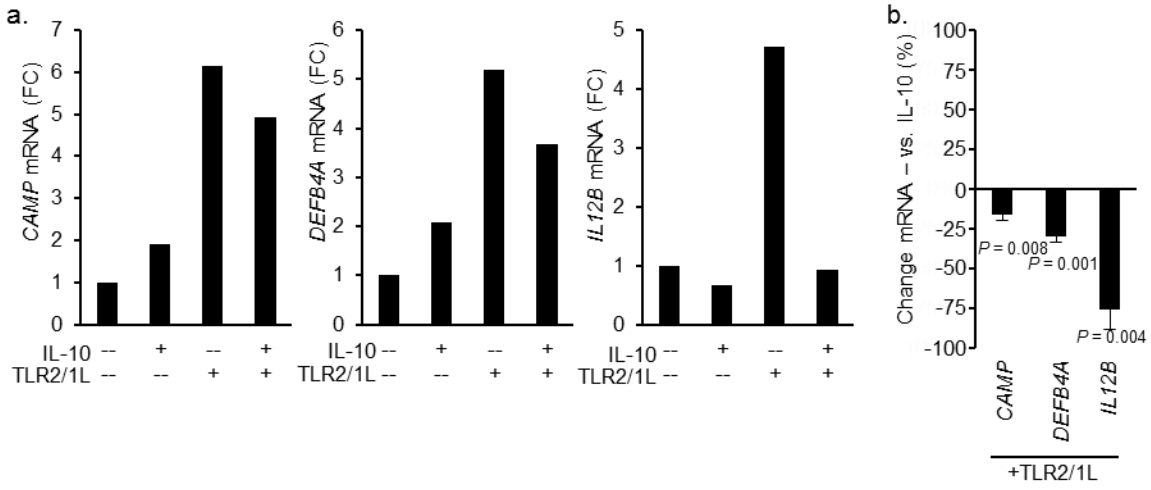

Supplemental Figure 7. Effect of exogenous IL-10 on TLR-induced antimicrobial expression. Expression levels by qPCR of *CAMP*, *DEFB4A* and *IL12B* in primary human monocytes treated with either recombinant IL-10, TLR2/1L or both. *IL12B* is a positive control for IL-10 mediated TLR2/1 inhibition. Data shown is (**a**) representative experiment and a (**b**) summary of all experiments, shown as mean percent change ± SEM in TLR2/1L stimulated cells (–– vs IL-10), $n = 3$.

Supplemental Figure 8

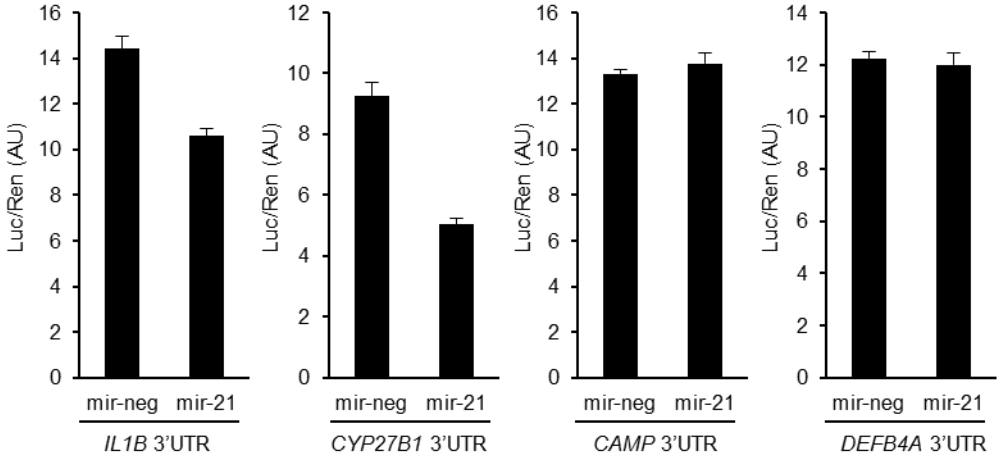

Supplemental Figure 8. Direct 3'UTR binding analysis. Luciferase activity normalized to the internal *Renilla* luciferase control activity of HEK-293 cells transfected with reporter constructs for the 3'UTR of *IL1B*, *CYP27B1*, *CAMP* or *DEFB4A*, with either mir-neg or mir-21 simultaneously. Data shown is representative of four to six independent experiments.

Supplemental Figure 9

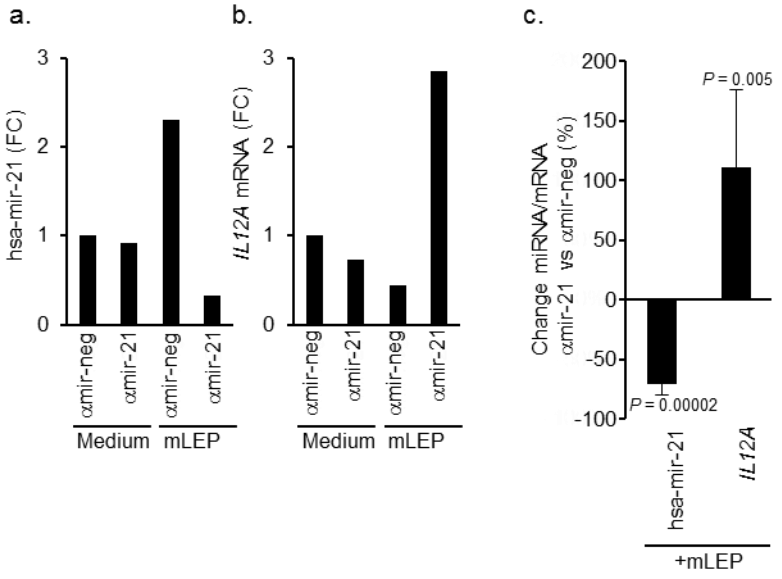

Supplemental Figure 9. Knockdown of hsa-mir-21 expression during *M. leprae* infection. Expression levels by qPCR of (**a**) hsa-mir-21 and (**b**) *IL12A* mRNA in primary human monocytes transfected with either a control anatgomir (αmir-neg) or an antagomir specific for hsa-mir-21 (αmir-21) followed by infection with *M. leprae* infection at MOI of ten. Data shown is (**a**-**b**) representative experiment and a (**c)** summary of all experiments, shown as mean percent change (αmir-neg vs αmir-21) ± SEM, *n* = 5-7.

Supplemental Figure 10

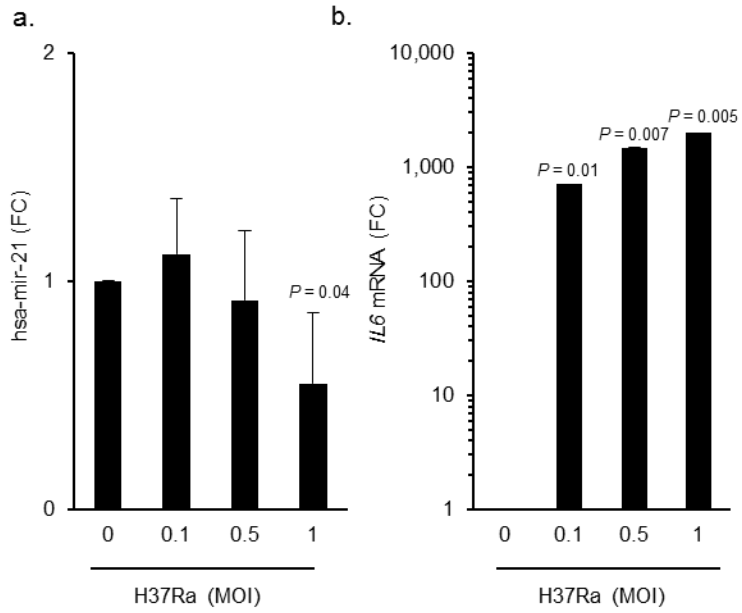

Supplemental Figure 10. Regulation of hsa-mir-21 by *M. tuberculosis*. Primary human monocytes were infected with *M. tuberculosis* H37Ra at MOI of 0.1, 0.5 and one for 18 h and the level of (**a**) hsa-mir-21 and (**b**) *IL6* mRNA was assessed by qPCR. Data shown is the mean fold change vs. MOI 0 ± SEM, *n* = 4-5.

Supplemental Figure 11

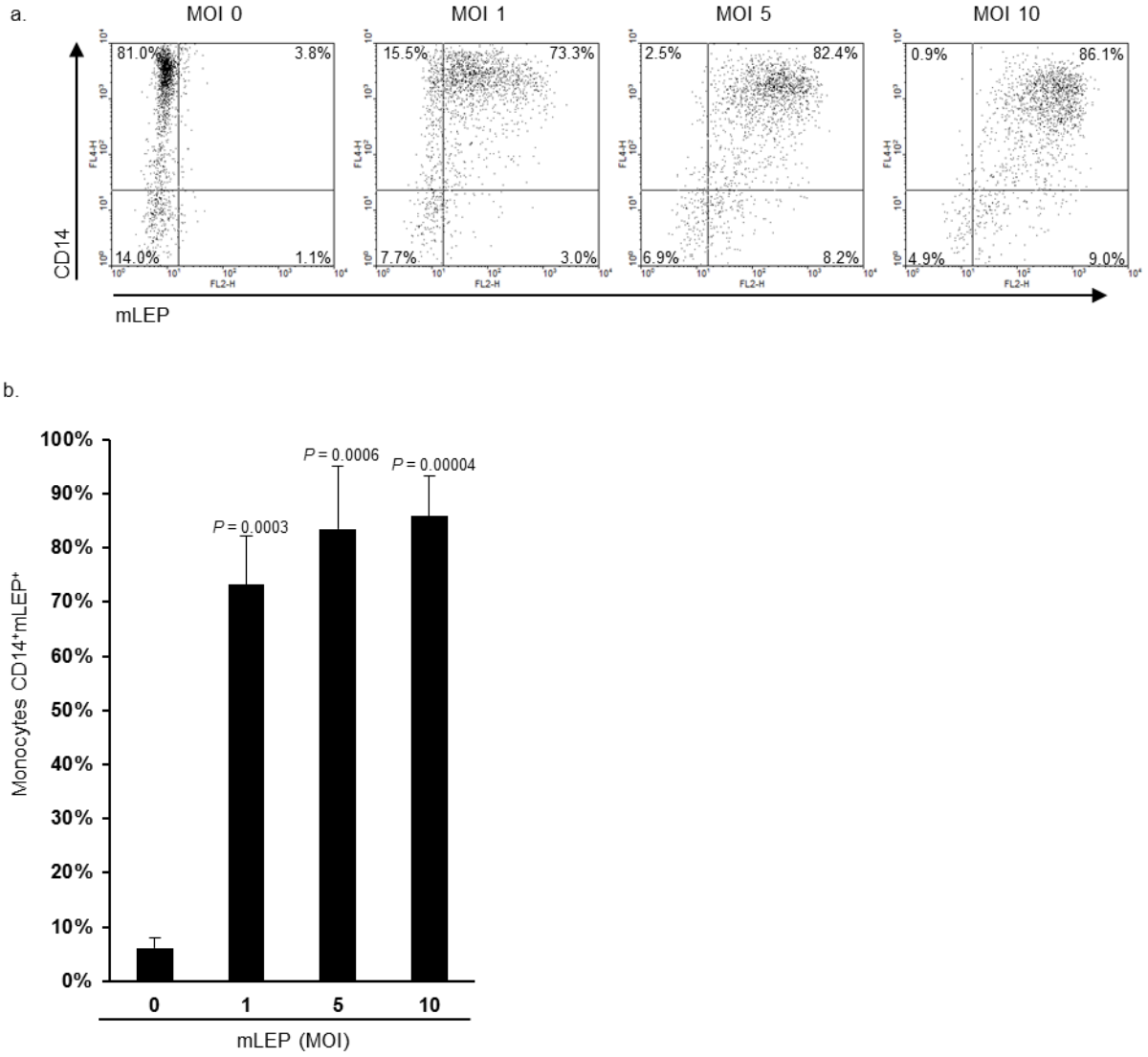

Supplemental Figure 11. *M. leprae* infection efficiency of primary human monocytes. Primary human monocytes were infected with PKH26-labeled live *M. leprae* at an MOI of one, five and ten for 18 h, and then co-labeled with a monoclonal antibody specific for CD14. Data shown is (**a**) representative of four individual donors, and (**b**) mean CD14 and *M. leprae* double positive cells ± SEM, $n = 4$.

Supplemental Figure 12

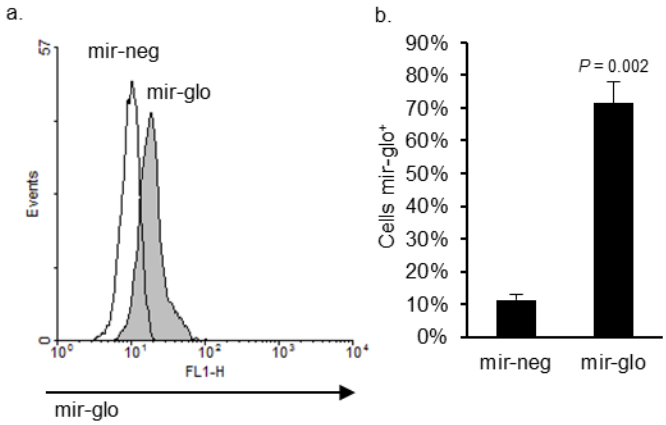

Supplemental Figure 12. Primary human monocyte transfection efficiency. Primary human monocytes were transfected with a Cy5-labeled non-targeting control miRNA oligo (mir-glo) or an unlabeled control oligo (mir-neg). Following transfection, the total mir-glo level in the transfected monocytes was evaluated using flow cytometry. Data shown is (**a**) representative of five donors, and (**b**) mean percent mir-glo positive cells ± SEM, $n = 5$.

SUPPLEMENTAL TEXT

Leprosy specific gene sets

L-lep specific gene list: interleukin 4 (*IL4*) [1-3], interleukin 5 (*IL5*) [1, 3], leukocyte immunoglobulin-like receptor, subfamily A (with TM domain), member 2 (*LILRA2*) [4], tumor necrosis factor (ligand) superfamily, member 13b (*TNFSF13B*) [4], transforming growth factor, beta 1 (*TGFB1*) [5], interleukin 10 (*IL10*) [1, 3], CD163 molecule (*CD163*) [6], peroxisome proliferator-activated receptor gamma (*PPARG*) [7], apolipoprotein E (*APOE*) [7], CD36 molecule (thrombospondin receptor) (*CD36*) [6], macrophage scavenger receptor 1 (*MSR1*) [6, 7], macrophage receptor with collagenous structure (*MARCO*) [6, 7], chemokine (C-X-C motif) ligand 16 (*CXCL16*) [6], oxidized low density lipoprotein (lectin-like) receptor 1 (*OLR1*) [6], scavenger receptor class B, member 1 (*SCARB1*) [6], CD68 molecule (*CD68*) [6].

T-lep specific gene list: interleukin 12A (*IL12A*) [8], interleukin 12B (*IL12B*) [8], interleukin 7 (*IL7*) [9], interleukin 18 (*IL18*) [10], signaling lymphocytic activation molecule family member 1 (*SLAMF1*) [4, 11], CD1b molecule (*CD1B*) [12, 13], colony stimulating factor 2 (granulocyte-macrophage) (*CSF2*) [3], colony stimulating factor 2 receptor, alpha, low-affinity (granulocyte-macrophage) (*CSF2RA*) [13, 14], CD40 molecule, TNF receptor superfamily member 5 (*CD40*) [15], CD40 ligand (*CD40L*) [15], interferon, gamma (*IFNG*) [1, 2], interleukin 15 (*IL15*) [2], interleukin 2 receptor, beta (*IL2RB*) [16], interleukin 2 receptor, gamma (*IL2RG*) [16], interleukin 1, beta (*IL1B*) [3], interleukin 1 receptor, type I (*IL1R1*) [4], cytochrome P450, family 27, subfamily B, polypeptide 1 (*CYP27B1*) [6], vitamin D (1,25- dihydroxyvitamin D3) receptor (*VDR*) [6], cytochrome P450, family 24, subfamily A, polypeptide 1 (*CYP24A1*) [6], granulysin (*GNLY*) [17].

Targeting preference score

The potential ability of the 468 annotated miRNA species represented on the microarray platform to target the 3'UTRs of the genes in the leprosy specific gene sets (defined above) were analyzed using the online database TargetScanHuman [18]. Given that the two leprosy specific gene sets have different numbers of genes, the targeting frequency of each individual miRNA species was calculated for the two sets of genes differentially expressed in T-lep and L-lep lesions. All miRNA species were ranked based on their 'targeting preference score', the degree of differential targeting of T-Lep versus L-lep signature genes (**Supplemental Fig. 2**). All miRNA species were rank ordered based on their targeting frequency score. This yielded three principal categories within the ranked list: i) preferentially targeting T-lep genes (preference score > 0), ii) no targeting preference (preference score = 0), and iii) preferentially targeting L-lep genes (preference score < 0).

The statistical significance of leprosy specific miRNA species enrichment was determined by 'Kolmogorov-Smirnov (KS)-based permutation analysis. Ranked lists annotated with the presence or absence of differential expression were scanned using all possible rank thresholds for the point of maximal enrichment as defined by the maximal KS distance. Permutation analysis was then performed by randomly reassigning the targeting preference scores used for ranking. The fraction of permutation cases resulting in a maximal KS distance greater than or equal to the observed maximum value was then defined as the permutation-based frequency of random occurrence, i.e. the permutation-based p-value. This procedure is analogous to the permutation approach used in Gene Set Enrichment Analysis (GSEA) [19]. Using this analysis the L-lep specific miRNA species were significantly enriched within the group of miRNA with a preference score greater than zero (**Fig. 1c**). In contrast the two T-lep specific miRNA species showed no statistical enrichment due to the lack of statistical power.

Direct 3'UTR binding

In order to ascertain if hsa-mir-21 directly regulated the expression of the key antimicrobial genes, the ability of hsa-mir-21 to bind the three prime untranslated region (3'UTR) of these genes was assessed. Constructs containing the firefly luciferase gene with the 3'UTR of the gene of interest driven by the CMV promoter were co-transfected with a non-targeting oligo or hsa-mir-21 into HEK-293 cells. Following transfection, the resulting firefly luciferase activity was measured, and normalized to activity of the internal *Renilla* luciferase control on the plasmids. Presence of hsa-mir-21 resulted in the downregulation of luciferase activity in cells transfected with the *IL1B* and *CYP27B1* 3'UTR constructs. In contrast, hsa-mir-21 had no effect on the luciferase activity in cell transfected with the *CAMP* and *DEFB4A* 3'UTR constructs (Representative Experiment, **Supplemental Fig. 8**). In these assays, hsa-mir-21 downregulated luciferase activity by 14% (P = 0.02) in the *IL1B* 3'UTR and 21% (P = 0.04) in the *CYP27B1* constructs (**Fig. 4d**). These data indicate that hsa-mir-21 directly regulates two key components of the vitamin D antimicrobial pathway, *IL1B* and *CYP27B1*, leading to downstream inhibition of antimicrobial peptide gene expression.

PCR-based bacterial viability

This PCR-based assay is a powerful tool for the investigation of *M. leprae* biology as well as other mycobacterial pathogens both *in vivo* and *in vitro*. Although *M. leprae* can also be assessed using radiorespiromtery and BacLight, these approaches were not feasible here as the cell yield after transfection was limiting. However, as demonstrated by Martinez *et al.*, the PCR-based assay is comparable to both radiorespirometry and BacLight in its ability to determine *M. leprae* viability [20]. In addition to *M. leprae*, similar PCR based methods have been used to assess the viability in vitro of *M. tuberculosis* [21] as well as *M. avium* [22]. Levels of *M. tuberculosis* 16S RNA and IS6110 have been previously explored as a measurement of *M. tuberculosis* viability in sputum samples *in vivo* following chemotherapy treatment in patients [23]. In this study, the authors found that in patient's sputum, *M. tuberculosis* 16S RNA levels

rapidly declined upon initiation of antimicrobial therapy, whereas IS6110 DNA levels remained constant, which mirrors the expected results of an *in vitro* viability assay for *M. tuberculosis*.

In our previous studies of siRNA transfected monocytes stimulated with TLR2/1L, examining antimicrobial effects against H37Ra, we demonstrated a significant ($P = 0.05$) TLR2/1L-induced antimicrobial activity of 14.5% ± 1.3 by the CFU assay [24]. These results are comparable to the data shown in this manuscript using the real time PCR method, where we demonstrate a significant ($P = 0.02$) TLR2/1L-induced antimicrobial activity against H37Ra in mir-neg transfected monocytes of 18.0% ± 0.08. Given the similarities between the nontargeting siRNA control used in the previous study and the mir-neg non-targeting control used here (both 21 nucleotides long, double stranded RNA oligos), we feel that these results demonstrate that the real time PCR assay is comparable to the CFU assay.

SUPPLEMENTAL METHODS

Reagents

Mature miRNA oligos and antagomir oligos were purchased (Applied Biosystems), resuspended in sterile DEPC-treated water at 20μM, stored in aliquots at 80°C, and used at 2.5μl per reaction. TLR2/1L is a synthetic 19kDa *M. tuberculosis* derived lipopeptide used at 10μg/ml (EMC Microcollections). Recombinant IFN-γ (BD Bioscience) and IL-10 (R&D Systems) were purchased and both used at 10ng/ml. Biotinylated LNA probes used for fluorescent in situ hybridization were purchased (Exiqon, Woburn, MA) and stored in small aliquots at -20°C. Strep-avidin horse radish peroxidase (*S*A-HRP, Thermo Fisher) was resuspended in DEPC-treated water at 1mg/ml, then stored in small aliquots at -20°C and diluted 1:2000 before use. miRNA Target Clones containing the 3'UTR of *IL1B*, *CYP27B1*, *CAMP* and *DEFB4* were purchased (Genecopoeia). HEK293 cells were purchased, and maintained according to the manufacturer's recommended conditions (ATCC). Human CD14 specific monoclonal antibody conjugated with APC was purchased and used as recommended by the manufacturer (BD Pharmingen).

Primer sequences

The following primers were designed: *IL6* Forward 5'-GAC CCA ACC ACA AAT GCC A-3', *IL6* Reverse 5'-CAT GTC CTG CAG CCA CTG G-3', *IL1B* Forward 5'-GCT TAT GTG CAC GAT GCA CC-3', *IL1B* Reverse 5'-GAG GCC CAA GGC CAC AG-3', *IL12A* Forward 5'-AGT GGA GGC CTG TTT ACC ATT GGA-3', *IL12A* Reverse 5'-AGG CCA GGC AAC TCC CAT TAG TTA-3', *IL10* Forward 5'-GAG AAC CAA GAC CCA GAC ATC AAG-3', *IL10* Reverse 5'-CAT TGT CAT GTA GGC TTC TAT GTA GTT G-3', hsa-mir-21 5'-CGG TAG CTT ATC AGA CTG ATG TTG A-3', and hsa-let-7c 5'-CGC TGA GGT AGT AGG TTG TAT GGT T-3'. For *M. tuberculosis*

H37Ra, the IS6110 genomic element was used and the primer sequences are as follows: 16S Forward 5'-GGT GCG AGC GTT GTC CGG AA-3', 16S Reverse 5'- CGC CCG CAC GCT CAC AGT TA-3', IS6110 Forward 5'-GGA AGC TCC TAT GAC AAT GCA CTA G-3', and IS6110 Reverse 5'-TCT TGT ATA GGC CGT TGA TCG TCT-3'.

Leprosy biopsy specimens

We have established a library of skin biopsy specimens collected from new untreated patients at the time of diagnosis from the Hansen's Disease Clinic at Los Angeles Country and University of Southern California Medical Center as well as the Leprosy Clinic at the Oswaldo Cruz Foundation in Brazil presenting between 2005-2010. The diagnosis and classification of patients was established by means of clinical and histopathological criteria of Ridley and Jopling [25]. T-lep patients were classified as borderline tuberculoid (BT) and L-lep patients classified as lepromatous (LL). For the microarray, qPCR and FISH studies presented here, skin biopsy specimens from T-lep and L-lep patients were randomly selected from the library, representing a total of 20 individual T-lep patients and 23 individual L-lep patients. Specimens were embedded in OCT medium, snap-frozen in liquid nitrogen and stored at -80°C until sectioning. Tissue sections were either mounted on slides for *in situ* hybridization or processed for RNA isolation.

Microarray analysis

Total RNA was isolated from six lepromatous and six tuberculoid leprosy lesions as previously described [13]. Data obtained from the miRNA analysis indicated that one lepromatous sample was to be excluded from further analysis due to low RNA quality. For the hierarchical clustering, the individual probe expression patterns were compared using a centered Pearson correlation coefficient. Cluster dendrograms were generated using the Cluster and TreeView software

programs from the Eisen Lab at http://rana.lbl.gov/ [26]. For heatmap-based visualization, expression values were mean subtracted with the sum of squares set equal to one [26].

Live *M. leprae*

M. leprae is grown in the footpad of nu/nu mice, harvested and treated with NaOH to remove mouse tissue, and the bacteria viability is assessed by determining the rate of palmitic acid oxidation, bacterial membrane integrity, and growth in the mouse footpad [27]. A portion of the *M. leprae* is then incubated with the fluorescent dye: PKH26. The NaOH treated *M. leprae* preps are shipped overnight at on ice, which was determined to have minimal impact on the bacteria viability.

Isolation and infection of monocytes

The collection and analysis of peripheral blood cells from healthy blood donors was approved by the committees on investigations involving human subjects of the University of California, Los Angeles, and all donors provided written informed consent. Mononuclear cells were isolated from peripheral blood of healthy donors using Ficoll-Paque as previously described [28]. Monocytes were purified by plastic adherence for two hours in RPMI 1640 (Invitrogen) supplemented with 1% fetal calf serum (Omega Scientific). Non-adherent cells were removed via vigorous washing and cultured in RPMI supplemented with antibiotics and 10% fetal calf serum, or 10% vitamin D-sufficient (100 nM) human serum for antimicrobial peptide gene expression studies or *M. leprae* infection studies. For *M. leprae* infection studies, monocytes were infected with single cell suspensions of *M. leprae* at a MOI of one, five, and ten then cultured at 33 °C for 18 or 40 h. Using PKH26-labled *M. leprae*, the infection efficiency of CD14 positive monocytes was determined using flow cytometry (**Supplemental Fig. 11a**), as previously described [24]. An average of 73%, 84% and 86% of monocytes in culture were *M. leprae* positive at a MOI of one, five, and ten, respectively (**Supplemental Fig. 11b**). At MOI

of ten, each infected cell contained an average of 2.1 ± 0.4 bacteria (average of three individual donors). Unless indicated, all experiments involving live *M. leprae* were conducted with a MOI of ten. For *M. tuberculosis* infection studies, monocytes were infected with single cell suspensions of *M. tuberculosis* H37Ra at a MOI of 0.1, 0.5 and one, and then cultured at 37 °C for 18 h, or with an MOI of 0.5 for transfected cells, as we previously described [24]. An MOI of 0.5 was optimized based on infectivity and viability of the transfected monocytes.

Quantitative PCR

For mRNA studies, the data was analyzed using the $\Delta\Delta C_T$ method as previously described [28] using *36B4* as the normalizer. The results are then calculated as a fold change to control treated cells. For miRNA studies, four different "normalizing" short RNA sequences were tested over several donors and experiments; however, none demonstrated sufficient stability for use as a qPCR normalizer, which corroborates published data [29]. Therefore, the samples were normalized to the same input cell number prior to applying the Cells-to-CT or NCODE kits, and analyzed using the ΔC_T method. The results are then calculated as a fold change to control cells.

Transfection of monocytes

Transfection efficiency was evaluated using the Cy5-labeled non-targeting miRNA oligo (mir-glo). Primary monocytes were transfected with mir-glo or an unlabeled control oligo (mir-neg), and mir-glo positive cells were assessed by flow cytometry (**Supplemental Fig. 12a**). In five independent experiments, the average number of mir-glo positive cells was 71% ± 6% (P = 0.002, **Supplemental Fig. 12b**). Following transfection, the cells were allowed to recover for two hours in the provided transfection medium, then washed and plated in RPMI and 10% FCS, or 10% pooled human vitamin D sufficient serum for the cathelicidin and DEFB4 studies. The

cells transfected with the mature miRNA oligos were then stimulated with TLR2/1L (10 μg ml^{-1}) incubated for either 18 or 24 hours. The antagomir transfected cells were infected with live *M. leprae* (MOI 10) as above and incubated for 18 to 24 h. Total RNA was harvested following the incubation and quantitative PCR was performed.

Cytometric bead array

Supernatants from the transfected and stimulated monocytes were harvested at 18 and 24 h. IL-1β, IL-10 and IL-6 cytokine levels in the supernatants were assessed using Cytometric Bead Array Flex Set (BD Biosciences) according to the manufacturer's recommended protocols. The beads were visualized using a BD FACSCalibur (BD Biosciences) and analyzed with Flowjo Software (Tree Star).

Antimicrobial assays

Monocytes were first transfected as indicated, and infected overnight with an MOI of ten for *M. leprae*, and an MOI of 0.5 with *M. tuberculosis* H37Ra, then counted and viability assessed using trypan blue exclusion. Higher MOIs of H37Ra were toxic to the transfected monocytes. The infected cells were cultured in equal amounts of viable cells for all conditions tested, followed by stimulation with the TLR2/1L or medium for three days as indicated above. Following the incubation, the cells are harvested and divided. Half of the cells were lysed by boiling at 100 °C for 5 min then snap freezing at -80 °C, and total RNA was isolated from the remaining half using Trizol as detailed above, followed by RNA cleanup and on column DNAse digestion using RNeasy Miniprep Kit (Qiagen). cDNA was synthesized from the total RNA as described above. The bacterial 16S rRNA, and genomic element DNA levels were then assessed using real time PCR as detailed above from the cDNA and cellular lysate, respectively. In order to normalize for the total monocytes present in the culture, *36B4* was also

evaluated, which were capable of amplifying the human genomic DNA. Comparison of the bacterial DNA to the mammalian *36B4* levels was used to monitor infectivity between all the conditions in the assay as well as PCR quality.

SUPPLEMENTAL REFERENCES

1. Yamamura,M. et al. Defining protective responses to pathogens: cytokine profiles in leprosy lesions. Science 254, 277-279 (1991).

2. Jullien,D. et al. IL-15, an immunomodulator of T cell responses in intracellular infection. J. Immunol. 158, 800-806 (1997).

3. Yamamura,M. et al. Cytokine patterns of immunologically mediated tissue damage. J. Immunol. 149, 1470-1475 (1992).

4. Bleharski,J.R. et al. Use of genetic profiling in leprosy to discriminate clinical forms of the disease. Science 301, 1527-1530 (2003).

5. Goulart,I.M., Figueiredo,F., Coimbra,T., & Foss,N.T. Detection of transforming growth factor-beta 1 in dermal lesions of different clinical forms of leprosy. Am. J. Pathol. 148, 911-917 (1996).

6. Montoya,D. et al. Divergence of macrophage phagocytic and antimicrobial programs in leprosy. Cell Host. Microbe 6, 343-353 (2009).

7. Cruz,D. et al. Host-derived oxidized phospholipids and HDL regulate innate immunity in human leprosy. J. Clin. Invest 118, 2917-2928 (2008).

8. Sieling,P.A. et al. IL-12 regulates T helper Type 1 cytokine responses in human infectious disease. J. Immunol. 153, 3639-3647 (1994).

9. Sieling,P.A. et al. IL-7 in the cell-mediated immune response to a human pathogen. J. Immunol. 154, 2775-2783 (1995).

10. Garcia,V.E. et al. IL-18 promotes type 1 cytokine production from NK cells and T cells in human intracellular infection. J Immunol 162, 6114-6121 (1999).

11. Garcia,V.E. et al. Signaling lymphocytic activation molecule expression and regulation in human intracellular infection correlate with Th1 cytokine patterns. J Immunol 167, 5719-5724 (2001).

12. Sieling,P.A. et al. CD1 expression by dendritic cells in human leprosy lesions: Correlation with effective host immunity. J Immunol 162, 1851-1858 (1999).

13. Krutzik,S.R. et al. TLR activation triggers the rapid differentiation of monocytes into macrophages and dendritic cells. Nat. Med. 11, 653-660 (2005).

14. Krutzik,S.R. et al. Activation and regulation of Toll-like receptors 2 and 1 in human leprosy. Nat. Med. 9, 525-532 (2003).

15. Yamauchi,P.S. et al. A role for CD40-CD40 ligand interactions in the generation of type 1 cytokine responses in human leprosy. J. Immunol. 165, 1506-1512 (2000).

16. Modlin,R.L. et al. In situ identification of cells in human leprosy granulomas with monoclonal antibodies to interleukin 2 and its receptor. J. Immunol. 132, 3085-3090 (1984).

17. Ochoa,M.T. et al. T-cell release of granulysin contributes to host defense in leprosy. Nat. Med. 7, 174-179 (2001).

18. Lewis,B.P., Burge,C.B., & Bartel,D.P. Conserved seed pairing, often flanked by adenosines, indicates that thousands of human genes are microRNA targets. Cell 120, 15-20 (2005).

19. Subramanian,A. et al. Gene set enrichment analysis: a knowledge-based approach for interpreting genome-wide expression profiles. Proc. Natl. Acad. Sci. U. S. A 102, 15545-15550 (2005).

20. Martinez,A.N. et al. Molecular determination of Mycobacterium leprae viability by use of real-time PCR. J. Clin. Microbiol. 47, 2124-2130 (2009).

21. Munoz-Elias,E.J. et al. Replication dynamics of Mycobacterium tuberculosis in chronically infected mice. Infect. Immun. 73, 546-551 (2005).

22. Kralik,P., Nocker,A., & Pavlik,I. Mycobacterium avium subsp. paratuberculosis viability determination using F57 quantitative PCR in combination with propidium monoazide treatment. Int J Food Microbiol. 141 Suppl 1, S80-S86 (2010).

23. Desjardin,L.E. et al. Measurement of sputum Mycobacterium tuberculosis messenger RNA as a surrogate for response to chemotherapy. Am J Respir. Crit Care Med 160, 203-210 (1999).

24. Liu,P.T. et al. Convergence of IL-1beta and VDR activation pathways in human TLR2/1-induced antimicrobial responses. PLoS. ONE. 4, e5810 (2009).

25. Ridley,D.S. & Jopling,W.H. Classification of leprosy according to immunity. A five-group system. Int. J. Lepr. 34, 255-273 (1966).

26. Eisen,M.B., Spellman,P.T., Brown,P.O., & Botstein,D. Cluster analysis and display of genome-wide expression patterns. Proc. Natl. Acad. Sci. U. S. A 95, 14863-14868 (1998).

27. Lahiri,R., Randhawa,B., & Krahenbuhl,J.L. Effects of purification and fluorescent staining on viability of Mycobacterium leprae. Int. J Lepr. Other Mycobact. Dis. 73, 194-202 (2005).

28. Liu,P.T. et al. Toll-like receptor triggering of a vitamin D-mediated human antimicrobial response. Science 311, 1770-1773 (2006).

29. Peltier,H.J. & Latham,G.J. Normalization of microRNA expression levels in quantitative RT-PCR assays: identification of suitable reference RNA targets in normal and cancerous human solid tissues. RNA. 14, 844-852 (2008).